The Electrochemical Society
Advancing solid state & electrochemical science & technology

A Computational Characterization of 2,2′-bis(trifluoromethyl)-[1,1′-biphenyl]-4,4′-diamine Iodine Dopant for Improving Power-Conversion Efficiency of Perovskite Solar Cells

View the article online for updates and enhancements.

A Computational Characterization of 2,2′-bis(trifluoromethyl)-[1,1′-biphenyl]-4,4′-diamine Iodine Dopant for Improving Power-Conversion Efficiency of Perovskite Solar Cells

Zdeněk Slanina,[1,z] Filip Uhlík,[2] Lai Feng,[3] and Ludwik Adamowicz[1]

[1]Department of Chemistry and Biochemistry, University of Arizona, Tucson, Arizona 85721-0041, United States of America
[2]Department of Physical and Macromolecular Chemistry, Charles University in Prague, Faculty of Science, 128 43 Praha 2, Czech Republic
[3]Soochow Institute for Energy and Materials Innovation (SIEMIS), Jiangsu Key Laboratory of Advanced Carbon Materials and Wearable Energy Technologies, School of Energy, Soochow University, Suzhou 215006, People's Republic of China

The paper presents ongoing density-functional theory (DFT) computational support to research of hybrid perovskite solar cells to facilitate their understanding at molecular level. Very recently, doping by a iodine salt, namely 2,2′-bis(trifluoromethyl)-[1,1′-biphenyl]-4,4′-diamine iodine $BFBAI_2$, has been described that improves the power conversion efficiency and enhances device stability. As structural characteristics of $BFBAI_2$ are not well known, they are supplied here through DFT calculations for both $BFBAI_2$ monomer and dimer. The geometry optimizations are performed at the M06-2X/3-21G level, and energetics is refined with the M06-2X/Def2QZVP treatment. The dimerization potential-energy change is calculated as -6.2 kcal/mol. $BFBAI_2$ exhibits highly non-uniform charge distribution, i.e., it is a clearly polar system that can strongly modulate surface conditions when adsorbed. The adsorption-energy gain for $BFBAI_2$ on $CsPbI_3$ perovskite is DFT evaluated as -13.2 kcal/mol.

Hybrid perovskite solar cells have been studied vigorously owing to their power conversion efficiency and other possible applications.[1–4] Very recently, doping by a iodine salt, namely 2,2′-bis(trifluoromethyl)-[1,1′-biphenyl]-4,4′-diamine iodine ($BFBAI_2$), has been reported[5] to improve the power conversion efficiency and to enhance device stability. However, structural characteristics of $BFBAI_2$ are poorly known and therefore they are supplied here through density-functional theory (DFT) modelling, actually for both $BFBAI_2$ monomer and dimer.

Calculations

The calculations for free $BFBAI_2$ were performed with the structures optimized in the standard 3-21G basis set,[6] using DFT approach, namely the M06-2X functional tested[7,8] as most reliable approximation for numerous application situations, including long-range interactions and hydrogen-bonded systems (i.e., the restricted M06-2X/3-21G treatment). The energetics was further refined using the standard Def2QZVP basis set[9] (M06-2X/Def2QZVP treatment).

In the optimized M06-2X/3-21G geometries, the harmonic vibrational analysis was carried out with the analytical force-constant matrix as a test that the true local energy minima were really localized,[10] and also for simulation of the vibrational spectra (in particular, for construction of vibrational partition functions in the rigid-rotor and harmonic-oscillator thermodynamic treatment[10]). The basis set superposition error (BSSE) was estimated by the Boys-Bernardi counterpoise (CP2) method.[11,12] The Boys-Bernardi counterpoise method is an approximative approach in order to ensure that each component of a chemical process, and especially of dimerizations, is treated with the same number of basis-set functions. This formal description is achieved via so called ghost atoms with no electrons. The BSSE problem originates in the finiteness of basis sets and it should disappear in a rather hypothetical case of an infinite basis set. All the computations were carried out with the Gaussian 09 program package.[13] The computations were performed in parallel regime, typically with 8-24 processors (up to 3 GHz each; the total internal memory up to 60 GB).

Finally, the adsorption of $BFBAI_2$ molecule on $CsPbI_3$ perovskite was treated with the gradient-corrected Perdew-Burke-Ernzerhof (PBE) functional[14] with double-zeta Gaussian basis sets[15] and Goedecker-Teter-Hutter (GTH) pseudopotentials[16] as implemented in the CP2K software package.[17] Starting from the experimentaly determined $CsPbI_3$ crystal structure, the geometry and cell parameters were optimized. The resulting unit cell was then replicated $4 \times 4 \times 3$ times and the resulting super-cell was doubled in the [001] direction to create a slab geometry. The $BFBAI_2$ molecule was placed near the surface comprising of Cs and I atoms and all coordinates (except 3 bottom layers of perovskite) were optimized.

Results and Discussion

Figures 1 and 2 show the M06-2X/3-21G optimized structures for the monomer and dimer of $BFBAI_2$, i.e., for the respective local energy minima confirmed by their vibrational analysis. Some selected optimized geometry parameters are given in Table I. The monomer exhibits the C_2 symmetry, and both species are chiral. In agreement with the findings for biphenyl,[18] the two connected benzene rings are distinctly non-coplanar which is a manifestation of repulsion between some of the groups when positioned in a close contact. On the other hand, there are also short contacts that contribute to stabilization of the dimer, namely C-F...H-N hydrogen bonds[19] with the two shortest F...H distances 1.86 and 1.87 Å (Fig. 2). Let us mention for completeness a kind of non-rigidity of the structures as they contain several rotating tops. Their internal rotation is relatively free[20] which is also seen in the values of the lowest calculated harmonic vibrational frequencies. In fact, the monomer exhibits 9 harmonic vibrational frequencies lower than $100\ cm^{-1}$ while in the dimer there are 20 such low vibrational frequencies.

Table II presents the Mulliken atomic charges on selected (electronegative) atoms together with dipole moments, thus pointing out a substantial variability of the charge distribution. The most negative charges appear on the nitrogen atoms, around -0.8 (of the elementary charge). Obviously, there have to be also carbon and hydrogen atoms in the systems with substantial positive charges. For example, in the $BFBAI_2$ monomer the highest positive charge amounts to $+0.388$ and $+0.894$ on the hydrogen and carbon atoms,
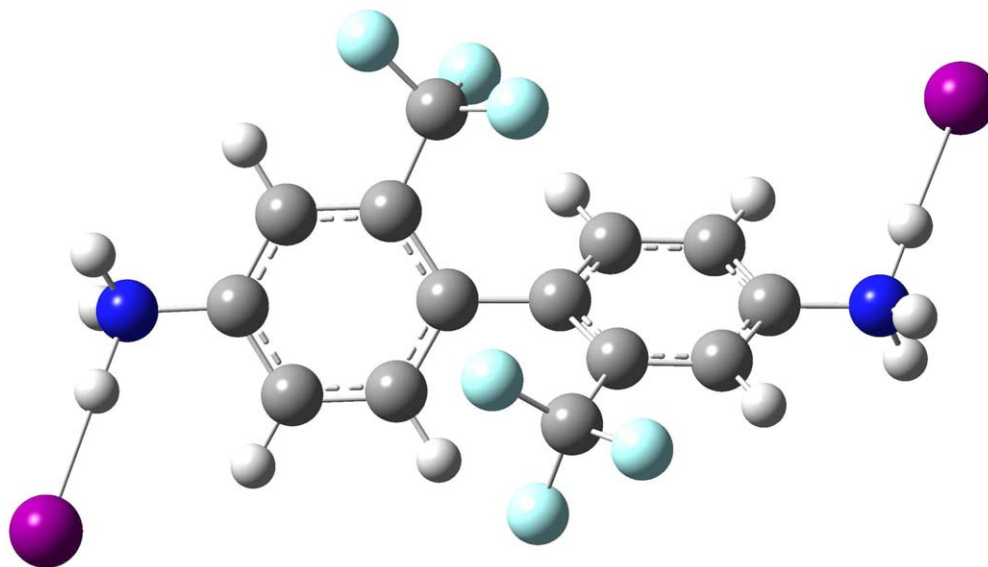
[z]E-mail: zdeneks@email.arizona.edu

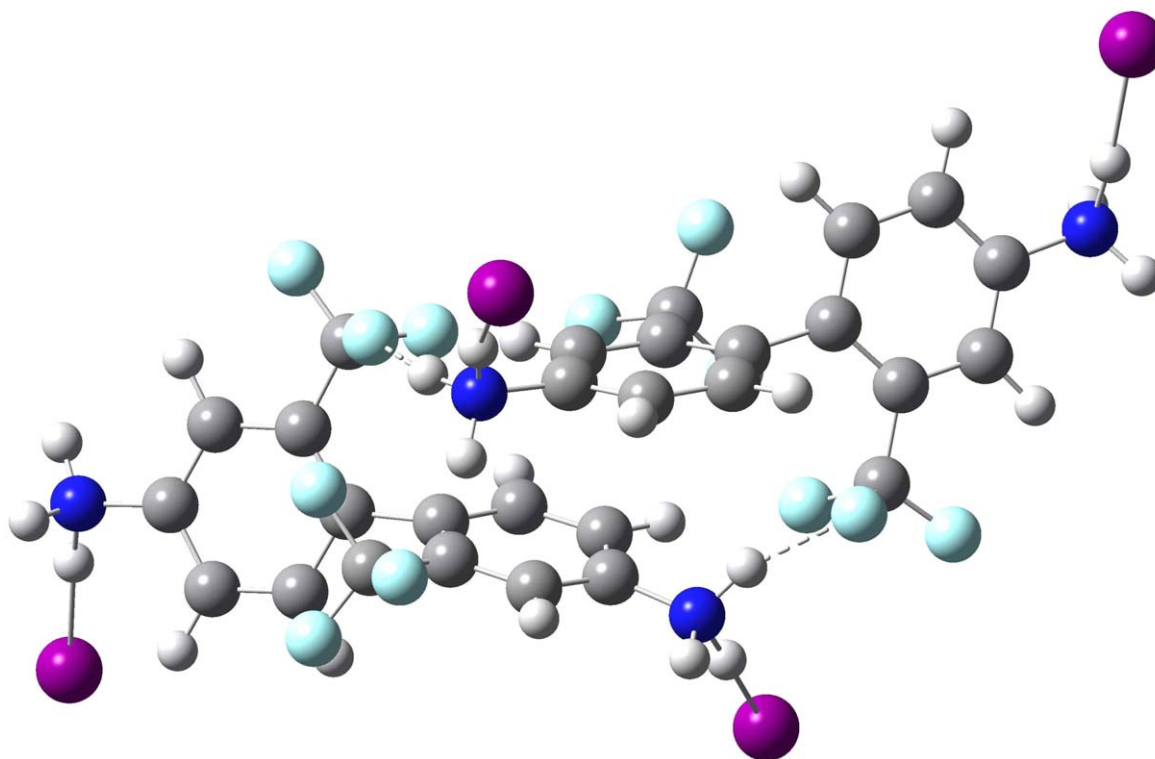**Figure 1.** The M06-2X/3-21G optimized structure of BFBAI$_2$.

Figure 2. The M06-2X/3-21G optimized structure of the BFBAI$_2$ dimer; dashed lines—the shortest H...F contacts: 1.87 Å(left), 1.86 Å(right).

Table I. **The average M06-2X/3-21G structural characteristics for monomer and dimer of BFBAI$_2$ –C –C bond connecting the benzene rings (Å), torsion angle between two benzene rings (deg), rotational constants *A*, *B*, *C* (GHz).**

Species	Symmetry	C–C	Torsion	*A*	*B*	*C*
Monomer (Fig. 1)	C_2	1.495	57.8	0.266 77	0.037 15	0.034 67
Dimer (Fig. 2)	C_1	1.498	73.5	0.037 52	0.014 04	0.012 47

respectively. Such pronounced charge distribution also leads to a relatively large dipole moment. It should be realized that the Mulliken atomic charges, owing to their definition, are to be derived from smaller basis sets like 3-21G. The Mulliken charges produced

by the 3-21G basis are known[21] to give a good agreement with the observed charges.[22] Moreover, there are general methodological arguments[23] why larger basis sets should not be used with the Mulliken charges as they can produce truly unreasonable values. It is

Table II. The average Mulliken atomic charges q_X on F, N, I atoms, and dipole moments (Debye) μ for monomer and dimer of BFBAI$_2$.

Species	q_F	q_N	q_I	μ
Monomer	−0.279	−0.806	−0.572	0.198
Dimer	−0.273	−0.817	−0.551	4.734

plausible to suppose that such polar molecules like BFBAI$_2$ can strongly modulate surface conditions when adsorbed. Figure 3 shows the M06-2X/Def2QZVP computed Raman and IR harmonic spectrum of the BFBAI$_2$ dimer. The spectra could in observation serve for documentation of the dimerization.

The calculated energy/enthalpy terms for the thermodynamic dimerization process:

$$2BFBAI_2(g) = (BFBAI_2)_2(g) \qquad [1]$$
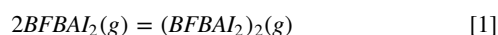
are surveyed in Table III. Calculated reaction thermodynamic changes are in literature mostly treated as the reaction potential-energy changes ΔE_{pot}. However, a more adequate approach deals[24] with the enthalpy change at absolute zero temperature $\Delta H_0°$, i.e., the potential-energy change corrected for the vibrational zero-point energies ZPE:

$$\Delta H_0° = \Delta E_{pot} + \Delta ZPE. \qquad [2]$$

The dimerization energy ΔE_{pot} or enthalpy $\Delta H°_0$ is refined here by inclusion of the basis set superposition error[11,12] (BSSE/CP2) (though so-called newly introduced steric correction[25] was not considered here). Interestingly, the values in Table III are not particularly method-dependent. In addition to the $\Delta H°_0$ term, also the dimerization enthalpy at room temperature $\Delta H°_{298.15}$ is presented, showing that the temperature dependence is not pronounced either. For comparison, one can recall the dimerization enthalpy $\Delta H°_{298.15}$ for water which is calculated,[26,27] in agreement with observations, around −3.5 kcal/mol. The dimerization of BFBAI$_2$ upon higher coverages can clearly represent an additional factor for the layer stabilization as well as for modulation of surface conditions.

The BSSE correction can reduce the energy gain significantly[28,29] and therefore it is an important refinement though not yet common for large systems. Still, the BSSE treatment itself is approximative. It can be avoided, for example, by using so called Gn methods,[30]
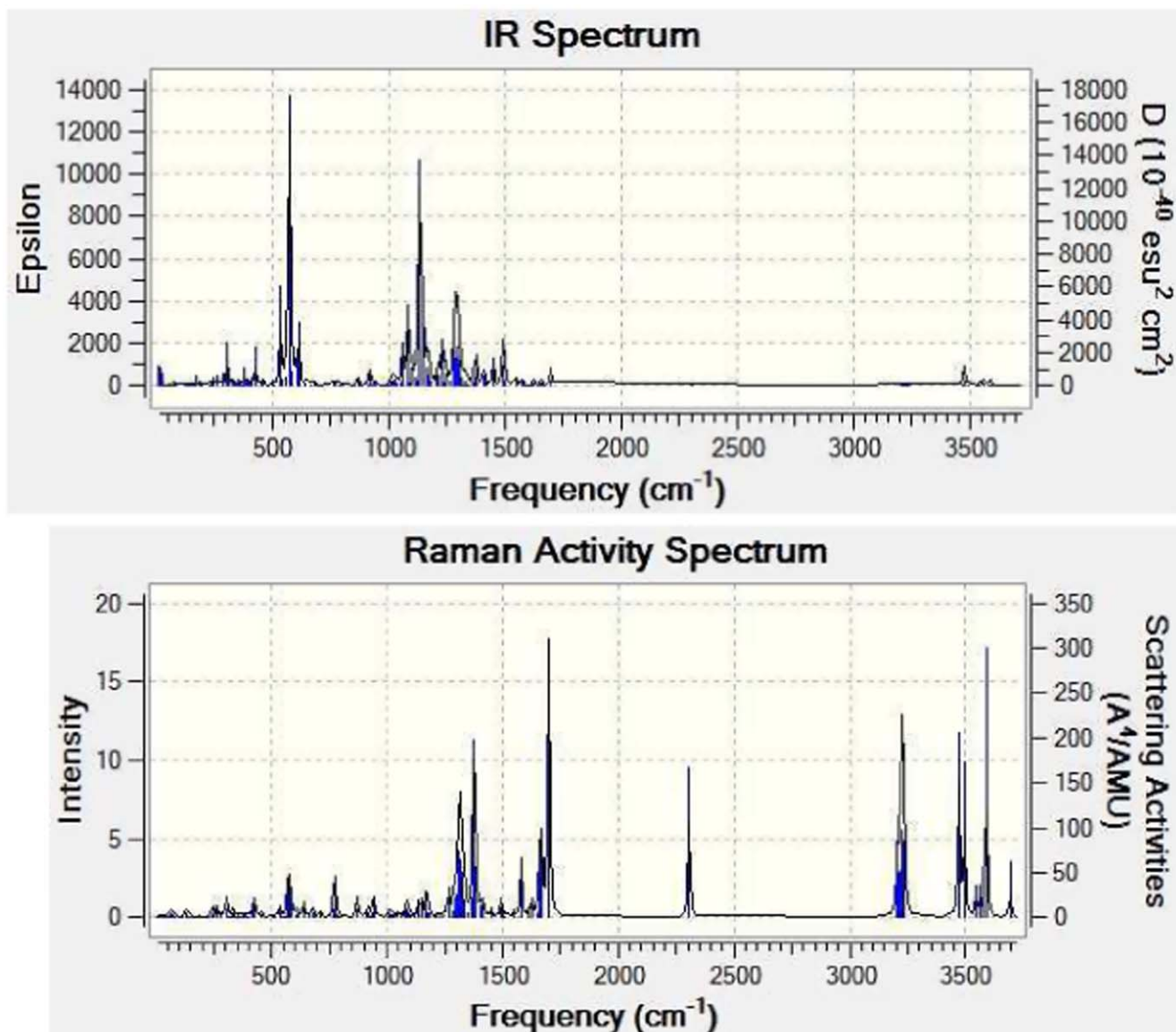

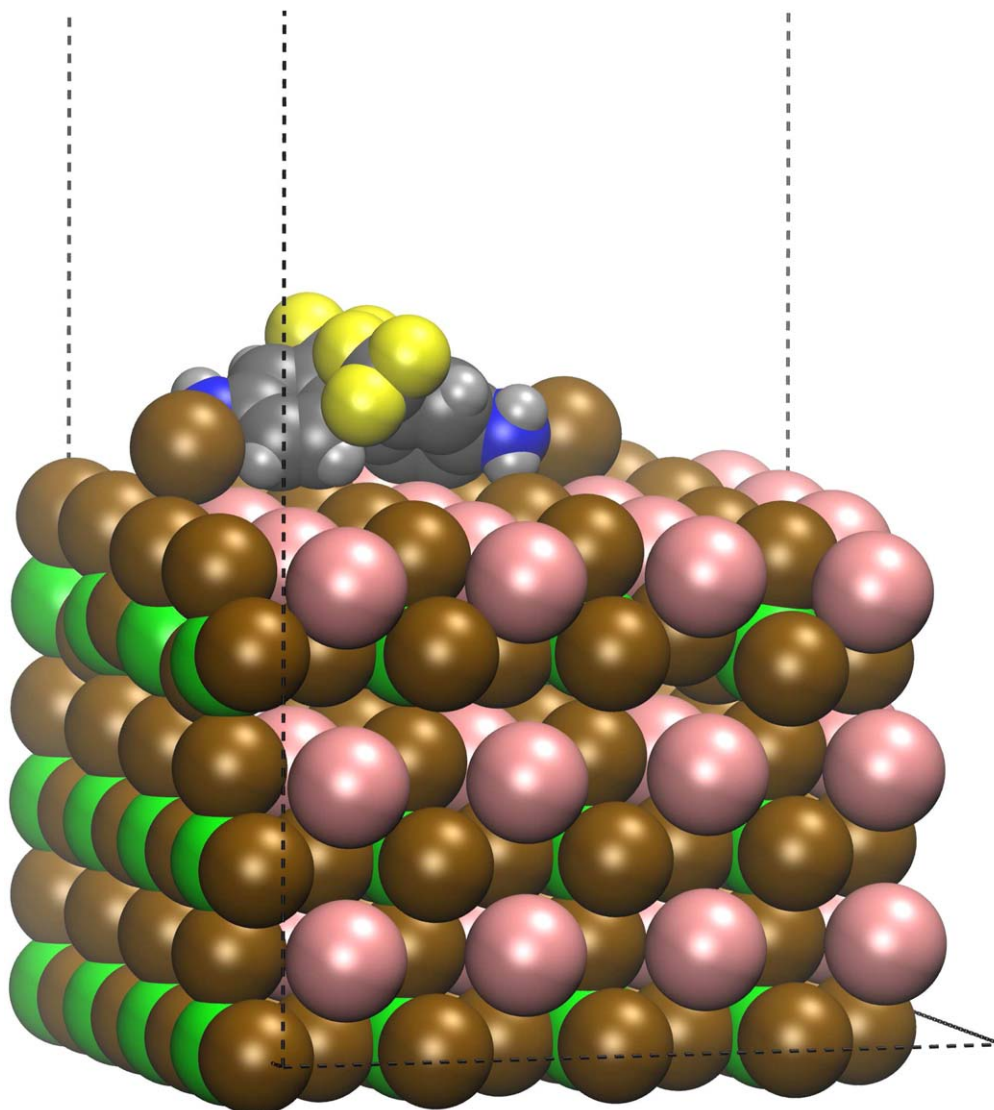**Figure 3.** M06-2X/Def2QZVP computed Raman and IR spectrum of the BFBAI$_2$ dimer.

Figure 4. Optimized structure of the BFBAI$_2$ molecule adsorbed on CsPbI$_3$ perovskite (Cs pink, Pb green, I brown, N blue, C black, H gray, F yellow).

Table III. The BFBAI$_2$ dimerization changes (kcal/mol) in potential energy ΔE_{pot}, enthalpy at absolute zero temperature ΔH_0°, and enthalpy at room temperature $\Delta H_{298.15}^\circ$.

Level	ΔE_{pot}	ΔH_0°	$\Delta H_{298.15}^\circ$
M06-2X/3-21G	−6.913	−6.830	−6.805
M06-2X/Def2QZVP	−6.190	−6.107	−6.081

however, only for relatively small systems. Gn methods include, inter alia, an approximative extrapolation toward infinite basis sets (i.e., basically toward the Hartree-Fock limit[31,32]). In particular, experience is lacking for estimation of the BSSE correction for solid-state systems. Nevertheless, we have tried to evaluate the adsorption energy of BFBAI$_2$ molecule on CsPbI$_3$ perovskite using Perdew-Burke-Ernzerhof functional.[14] The resulting optimized geometry is shown in Fig. 4, the calculated adsorption energy amounts to −13.2 kcal/mol. The chemically incompatible trifluoromethyl groups are rotated to vacuum while the hydrogen iodides dissociate protonating the amino groups with iodide anions located near cesium atoms. This corresponds to the known usual dissociation of hydrogen iodides of amino compounds as can be found in the crystallographic structural databases.

Further computational efforts are still needed in order to understand better such relatively complex new systems. A still deeper insight into observed phenomena supplied by calculations can help the search for even more efficient[33] energy-conversion perovskite systems.

ORCID

Zdeněk Slanina https://orcid.org/0000-0003-0292-9350

References

1. Q. Zeng, X. Zhang, C. Liu, T. Feng, Z. Chen, W. Zhang, W. Zheng, H. Zhang, and B. Yang, *Sol. RRL*, **3**, 1800239 (2019).
2. T.-C. Sum and N. Mathews (ed.), *Halide Perovskites: Photovoltaics, Light Emitting Devices, and Beyond* (Wiley-VCH, Weinheim) (2019).

3. M. Zhang, W. Hu, Y. Shang, W. Zhou, W. Zhang, and S. Yang, *Sol. RRL*, **4**, 2000113 (2020).
4. W. Zhao, S.-N. Hsu, B. W. Boudouris, and L. Dou, *ACS Appl. Electron. Mater.*, **3**, 5155 (2021).
5. D. Han, Q. Yuan, Z. Slanina, X. Tang, S. Yi, D.-Y. Zhou, F. Uhlik, and L. Feng, *Sol. RRL*, **5**, 2000629 (2021).
6. J. S. Binkley, J. A. Pople, and W. J. Hehre, *J. Am. Chem. Soc.*, **102**, 939 (1980).
7. Y. Zhao and D. G. Truhlar, *Theor. Chem. Acc.*, **120**, 215 (2008).
8. Y. Zhao and D. G. Truhlar, *Acc. Chem. Res.*, **41**, 157 (2008).
9. F. Weigend and R. Ahlrichs, *Phys. Chem. Chem. Phys.*, **7**, 3297 (2005).
10. Z. Slanina, *Contemporary Theory of Chemical Isomerism* (Academia and D. Reidel Publ. Comp., Prague and Dordrecht) p 47,164 (1986).
11. S. F. Boys and F. Bernardi, *Mol. Phys.*, **19**, 553 (1970).
12. F. B. van Duijneveldt, J. G. C. M. van Duijneveldt-van de Rijdt, and J. H. van Lenthe, *Chem. Rev.*, **94**, 1873 (1994).
13. M. J. Frisch et al., *Gaussian 09, Rev. C.01* (Gaussian Inc., Wallingford, CT) (2013).
14. J. P. Perdew, K. Burke, and M. Ernzerhof, *Phys. Rev. Lett.*, **77**, 3865 (1996).
15. J. VandeVondele and J. Hutter, *J. Chem. Phys.*, **127**, 114105 (2007).
16. S. Goedecker, M. Teter, and J. Hutter, *Phys. Rev. B*, **54**, 1703 (1996).
17. T. D. Kühne et al., *J. Chem. Phys.*, **152**, 194103 (2020).
18. M. P. Johansson and J. Olsen, *J. Chem. Theory Comput.*, **4**, 1460 (2008).
19. S. R. Chaudhari, S. Mogurampelly, and N. Suryaprakash, *J. Phys. Chem. B*, **117**, 1123 (2013).
20. Z. Slanina, *J. Phys. Chem.*, **86**, 4782 (1982).
21. Z. Slanina, F. Uhlík, S. Nagase, T. Akasaka, L. Adamowicz, and X. Lu, *Molecules*, **22**, 1053 (2017).
22. M. Takata, E. Nishibori, M. Sakata, and H. Shinohara, *New Diam. Front. Carb. Technol.*, **12**, 271 (2002).
23. F. Jensen, *Introduction to Computational Chemistry* (Wiley, Chichester) p 319 (2017).
24. Z. Slanina, F. Uhlík, C. Pan, T. Akasaka, X. Lu, and L. Adamowicz, *Chem. Phys. Lett.*, **710**, 147 (2018).
25. Z. Slanina, F. Uhlík, S.-L. Lee, L. Adamowicz, T. Akasaka, and S. Nagase, *Int. J. Quant. Chem.*, **111**, 2712 (2011).
26. Z. Slanina, F. Uhlík, X. Lu, T. Akasaka, K. H. Lemke, T. M. Seward, S. Nagase, and L. Adamowicz, *Fulleren. Nanotub. Carb. Nanostruct.*, **24**, 1 (2016).
27. F. Uhlík, Z. Slanina, S.-L. Lee, B.-C. Wang, L. Adamowicz, and S. Nagase, *J. Comput. Theor. Nanosci.*, **12**, 959 (2015).
28. Z. Slanina and S. Nagase, *Mol. Phys.*, **104**, 3167 (2006).
29. Z. Slanina, F. Uhlík, S. Nagase, T. Akasaka, X. Lu, and L. Adamowicz, *Chem. Phys. Lett.*, **695**, 245 (2018).
30. L. A. Curtiss, P. C. Redfern, and K. Raghavachari, *J. Chem. Phys.*, **126**, 084108 (2007).
31. F. Jensen, *Theor. Chem. Acc.*, **113**, 267 (2005).
32. A. Karton and J. M. L. Martin, *Theor. Chem. Acc.*, **115**, 330 (2006).
33. X. Zhu, *Acc. Chem. Res.*, **49**, 355 (2016).